

TABLE I. Half-width in polycrystals.

	Present paper $\lambda=3.0$ cm	Cummerow ¹ $\lambda=3.2$ cm	Zavoisky (in Van Vleck's paper)	Calc. width by dipolar broadening (Van Vleck)
MnSO ₄ ·5H ₂ O	1250 oersteds
MnSO ₄ ·4H ₂ O	1140	415	400	1500
MnSO ₄ ·H ₂ O	305
MnSO ₄	655	...	300	3500
CuSO ₄ ·5H ₂ O	300	318		
CuSO ₄ ·H ₂ O	310	...		
CuSO ₄	no absorption			

be applied here because the measured g -values in single crystals of tetrahydrates are almost constant in all orientations.

It is noticeable that, although the half-width of MnSO₄·5H₂O is about four times larger than that of CuSO₄·5H₂O, they are almost equal in the case of MnSO₄·H₂O and CuSO₄·H₂O. These differences may be ascribed to the different states of Mn²⁺ and Cu²⁺ ions, as the corresponding crystals have almost the same crystal structure.

The value of maximum χ'' per ion in the four states are shown in Table II.

TABLE II.

	MnSO ₄ ·5H ₂ O	MnSO ₄ ·4H ₂ O	MnSO ₄ ·H ₂ O	MnSO ₄
χ''/ion	0.56×10^{-25}	0.84×10^{-25}	1.97×10^{-25}	0.98×10^{-25}

The microwaves were generated by a demountable klystron continuously evacuated by an oil diffusion pump. The absorption was measured by the change of transmitted power through a resonant cavity containing the sample, the cavity being always kept at resonance. The incident power was monitored by a directional coupler, and the magnetic field was measured by proton resonance. Our thanks are due to Professor T. Mutō and Professor M. Kotani for valuable discussions.

* Now at Department of Physics, Faculty of Science, Kanazawa University.

† Department of Chemistry, Faculty of Science, Osaka University, Osaka, Japan.

¹ Cummerow, Halliday and Moore, Phys. Rev. **72**, 1233 (1947).

² J. H. Van Vleck, Phys. Rev. **74**, 1168 (1948).

Forbidden Beta-Ray Spectra

A. M. SMITH

Department of Natural Philosophy, University of Aberdeen,
Aberdeen, Scotland

(Received April 12, 1951)

RECENT developments in the study of shapes of forbidden beta-ray spectra have indicated that the interaction responsible for beta-decay may involve some linear combination of the five relativistically invariant forms which have hitherto been used.¹ (S , V , T , A , and P in the usual notation.) These developments are:

(a) The explanation of the shape of the spectrum of Cl³⁶ using a combination of interactions.²

(b) The explanation of the shapes of a number of spectra, (e.g., Sr⁸⁹, Sr⁹⁰, Y⁹⁰, Y⁹¹) using the α -factor.³ This implies a first-forbidden transition with the tensor or axial vector form of interaction, and would not be affected by using a combination of interactions. (It would be affected by a combination of the tensor and axial vector forms, but this combination is already excluded on other grounds.)⁴

(c) The explanation of the shape of the spectrum of Be¹⁰ using the D_2 factor,⁵ and of K⁴⁰ using the C factor.⁶ Neither of these would be affected by a combination of interactions.

In view of this, the cross correction factors for first- and second-forbidden transitions, which arise due to squaring of terms in the

interaction, have been worked out and are given here, as they may be of interest to others who are engaged in comparing observed spectra with theoretical predictions. Fierz⁴ has shown from consideration of the effect on the allowed spectrum that combinations of S with V and T with A must be excluded. We take as the invariant

$$I = \lambda_S S + \lambda_V V + \lambda_T T + \lambda_A A + \lambda_P P$$

with the understanding that $\lambda_S \lambda_V = \lambda_T \lambda_A = 0$. Using the same notation and method as in reference (1), the first-forbidden cross correction factors are:

$$C_{ST^1} = i\lambda_S \lambda_T \left[\left\{ \left(\int \mathbf{r} \right)^* \cdot \int \boldsymbol{\sigma} \times \mathbf{r} - \text{c.c.} \right\} (L_1 - M_0) - \left\{ \left(\int \mathbf{r} \right)^* \cdot \int \boldsymbol{\alpha} - \text{c.c.} \right\} \left(\frac{1}{3} K L_0 + N_0 \right) \right],$$

$$C_{SA^1} = -i\lambda_S \lambda_A \left[\left\{ \left(\int \mathbf{r} \right)^* \cdot \int \boldsymbol{\sigma} \times \mathbf{r} - \text{c.c.} \right\} \left(\frac{2}{3} K N_0^- + L_1^- + M_0^- \right) \right],$$

$$C_{VT^1} = \lambda_V \lambda_T \left[i \left\{ \left(\int \mathbf{r} \right)^* \cdot \int \boldsymbol{\alpha} - \text{c.c.} \right\} \left(\frac{1}{3} K L_0^- - N_0^- \right) + i \left\{ \left(\int \mathbf{r} \right)^* \cdot \int \boldsymbol{\sigma} \times \mathbf{r} - \text{c.c.} \right\} \left(\frac{2}{3} K N_0^- - L_1^- - M_0^- \right) - \left\{ \left(\int \boldsymbol{\alpha} \right)^* \cdot \int \boldsymbol{\sigma} \times \mathbf{r} + \text{c.c.} \right\} \times \left(\frac{1}{3} K L_0^- - N_0^- \right) + 2L_0^- \left| \int \boldsymbol{\alpha} \right|^2 \right],$$

$$C_{VA^1} = \lambda_V \lambda_A \left[i \left\{ \left(\int \mathbf{r} \right)^* \cdot \int \boldsymbol{\sigma} \times \mathbf{r} - \text{c.c.} \right\} (L_1 - M_0) + \left\{ \left(\int \boldsymbol{\alpha} \right)^* \cdot \int \boldsymbol{\sigma} \times \mathbf{r} + \text{c.c.} \right\} \left(\frac{1}{3} K L_0 + N_0 \right) \right],$$

$$C_{TP^1} = -i\lambda_T \lambda_P \left[\left\{ \left(\int \boldsymbol{\sigma} \cdot \mathbf{r} \right)^* \int \gamma_5 - \text{c.c.} \right\} \left(\frac{1}{3} K L_3 + N_0 \right) \right],$$

$$C_{AP^1} = \lambda_A \lambda_P \left[i \left\{ \left(\int \boldsymbol{\sigma} \cdot \mathbf{r} \right)^* \int \gamma_5 - \text{c.c.} \right\} \times \left(\frac{1}{3} K L_0^- - N_0^- \right) + 2L_0^- \left| \int \gamma_5 \right|^2 \right].$$

The second-forbidden cross correction factors are:

$$C_{ST^2} = i\lambda_S \lambda_T \left[\left\{ \sum_{ij} R_{ij}^* T_{ij} - \text{c.c.} \right\} \left\{ \frac{1}{6} K^2 (L_1 - M_0) + \frac{1}{3} (L_2 - M_1) \right\} - \left\{ \sum_{ij} R_{ij}^* A_{ij} - \text{c.c.} \right\} \times \left\{ (1/30) K^3 L_0 + \frac{1}{6} K^2 N_0 + \frac{1}{2} K L_1 + \frac{1}{3} N_1 \right\} \right],$$

$$C_{SA^2} = -i\lambda_S \lambda_A \left[\left\{ \sum_{ij} R_{ij}^* T_{ij} - \text{c.c.} \right\} \left\{ (1/15) K^3 N_0^- + \frac{1}{6} K^2 (L_1^- + M_0^-) + K N_1^- + \frac{1}{3} (L_2^- + M_1^-) \right\} \right],$$

$$C_{VT^2} = \lambda_V \lambda_T \left[i \left\{ \sum_{ij} R_{ij}^* T_{ij} - \text{c.c.} \right\} \times \left\{ (1/15) K^3 N_0^- - \frac{1}{6} K^2 (L_1^- + M_0^-) + K N_1^- - \frac{1}{3} (L_2^- + M_1^-) \right\} + i \left\{ \sum_{ij} R_{ij}^* A_{ij} - \text{c.c.} \right\} \times \left\{ (1/30) K^3 L_0^- - \frac{1}{6} K^2 N_0^- + \frac{1}{2} K L_1^- - \frac{1}{3} N_1^- \right\} - \frac{1}{4} \left\{ \sum_{ij} A_{ij}^* T_{ij} + \text{c.c.} \right\} \times \left\{ (1/15) K^3 L_0^- - \frac{1}{6} K^2 N_0^- + K L_1^- - 3N_1^- \right\} + \sum_{ij} |A_{ij}|^2 \left\{ \frac{1}{6} K^2 L_0^- + \frac{1}{3} L_1^- \right\} \right],$$

$$C_{VA^2} = \lambda_V \lambda_A \left[i \left\{ \sum_{ij} R_{ij}^* T_{ij} - \text{c.c.} \right\} \left\{ \frac{1}{6} K^2 (L_1 - M_0) + \frac{1}{3} (L_2 - M_1) \right\} + \frac{1}{4} \left\{ \sum_{ij} A_{ij}^* T_{ij} + \text{c.c.} \right\} \times \left\{ (1/15) K^3 L_0 + \frac{1}{6} K^2 N_0 + K L_1 + 3N_1 \right\} \right],$$

$$C_{VP^2} = -i\lambda_V \lambda_P \left[\left\{ \left(\int \boldsymbol{\alpha} \times \mathbf{r} \right)^* \cdot \int \gamma_5 \mathbf{r} - \text{c.c.} \right\} \times \left\{ \frac{2}{3} K N_0^- + L_1^- + M_0^- \right\} \right].$$

The L , M , and N functions are as given in reference 1, but because of the presence of the Dirac matrix β in some of the interactions and not in others, further functions L^- , M^- , and N^- have to be introduced. These are given below, and following the arrow in each case is an approximation good for $\alpha Z \ll 1$.

$$L_0^- = \left(\frac{2\pi}{F\rho^2}\right) \frac{g_0^2 - f_{-2}^2}{4\pi} = \frac{S+S^2}{2W} \rightarrow \frac{1}{W},$$

$$L_1^- = \left(\frac{2\pi}{F\rho^2}\right) \frac{g_1^2 - f_{-3}^2}{4\pi\rho^2} = \frac{F_1}{F} \frac{\rho^2}{9W} \frac{2S_1+S_1^2}{8} \rightarrow \frac{\rho^2}{9W},$$

$$L_2^- = \left(\frac{2\pi}{F\rho^2}\right) \frac{g_2^2 - f_{-4}^2}{4\pi\rho^4} = \frac{F_2}{F} \frac{\rho^4}{225W} \frac{3S_2+S_2^2}{18} \rightarrow \frac{\rho^4}{225W},$$

$$M_0^- = \left(\frac{2\pi}{F\rho^2}\right) \frac{f_0^2 - g_{-2}^2}{4\pi\rho^2}$$

$$= \frac{1}{W} \left[\frac{S-S^2}{2\rho^2} - \frac{\alpha Z W}{\rho} (1-S) \right]$$

$$+ \frac{1}{(2S+1)^2} \left\{ \rho^2(4S^4 - 7S^2 + 2) - \alpha^2 Z^2(4S^2 - S - 2) \right\}$$

$$\rightarrow \frac{1}{W} \left[\frac{\alpha^2 Z^2}{4\rho^2} - \frac{\rho^2}{9} \right],$$

$$M_1^- = \left(\frac{2\pi}{F\rho^2}\right) \frac{f_1^2 - g_{-3}^2}{4\pi\rho^4}$$

$$= \frac{F_1}{F} \frac{\rho^2}{36W} \left[\frac{2S_1 - S_1^2}{2\rho^2} - \frac{\alpha Z W}{\rho} (2 - S_1) \right]$$

$$- \frac{1}{(2S_1+1)^2(1+S_1)} \left\{ \frac{\rho^2}{2} (1+S_1)(4+4S_1+3S_1^2-2S_1^3) \right.$$

$$\left. + \frac{\alpha^2 Z^2}{2} (1+S_1) + \frac{\alpha^2 Z^2 W^2}{2} (8S_1^3 - 2S_1^2 - 21S_1 - 11) \right\}$$

$$\rightarrow \frac{\rho^2}{36W} \left[\frac{\alpha^2 Z^2}{4\rho^2} - \frac{4\rho^2}{25} \right],$$

$$N_0^- = \left(\frac{2\pi}{F\rho^2}\right) \frac{f_0 g_0 + f_{-2} g_{-2}}{4\pi\rho} = - \left[\frac{\alpha Z S}{2\rho W} - \alpha^2 Z^2 \right] \rightarrow - \frac{\alpha Z}{2\rho W},$$

$$N_1^- = \left(\frac{2\pi}{F\rho^2}\right) \frac{f_1 g_1 + f_{-3} g_{-3}}{4\pi\rho^3} = - \frac{F_1}{F} \frac{\rho^2}{36} \left[\frac{\alpha Z S_1}{2\rho W} - \alpha^2 Z^2 \right] \rightarrow - \frac{\rho^2 \alpha Z}{36\rho W}.$$

Work in connection with the comparison of complete correction factors with experimental spectra is proceeding.

¹ E. J. Konopinski and G. E. Uhlenbeck, *Phys. Rev.* **60**, 308 (1941).
² Longmire, Wu, and Townes, *Phys. Rev.* **76**, 693 (1949).
³ L. M. Langer and H. C. Price, *Phys. Rev.* **76**, 641 (1949).
⁴ M. Fierz, *Z. Physik* **104**, 553 (1936).
⁵ H. W. Fulbright and J. C. D. Milton, *Phys. Rev.* **76**, 1271 (1949).
⁶ D. E. Alburger, *Phys. Rev.* **78**, 629 (1950).

Magneto-Optics of an Electron Gas with Guided Microwaves*

L. GOLDSTEIN, M. LAMPERT, AND J. HENEY
Federal Telecommunication Laboratories, Inc., Nulley, New Jersey
 (Received April 17, 1951)

IN recent years the magneto-optics of electromagnetic wave propagation have been extended to guided propagation at microwave frequencies. In particular, Faraday-effect experiments have been made¹⁻³ in which the plane of maximum E -field of the TE_{11} mode in a circular wave guide is rotated by propagation through a section of the guide filled with a liquid or solid dielectric and located in an axial dc magnetic field. In all the published work to date, very small angles of rotation are obtained per guide wavelength, even at the gyromagnetic resonant field.

We have performed magneto-optic propagation experiments in circular wave guide in the range of frequencies 4600-5500 Mc/sec, employing as the dielectric the decaying plasma from a pulsed dc gas discharge. The main results are as follows:

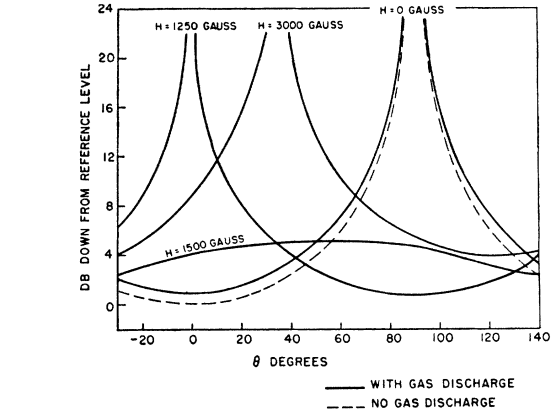


FIG. 1. Relative rf electric field distribution over periphery of circular wave guide. (Signal frequency: 5500 Mc/sec, Gas: Ne+1% at 1 mm Hg.) The reference plane for θ and the reference level for the E -field measurements are the plane and amplitude, respectively, of the maximum E -field with no discharge. Signal pulse 50 sec after 5 sec dc discharge pulse. Pulse voltage: 1050-v peak. Pulse current: 135-ma peak.

(1) Very large angles of rotation, on the order of 90° or more per guide wavelength, exhibiting a pronounced resonance behavior in the region where the gyromagnetic frequency of the electrons approaches the signal frequency.

(2) Departure from linear polarization as resonance is approached. Polarization becomes more broadly elliptical and finally almost purely circular at resonance.

(3) Demonstration of an analogue, for guided microwaves, of the crossed Nicol prisms experiment.

The anisotropic electron gas is produced by a pulsed dc discharge in a hot-cathode tube containing a rare gas, which completely fills a five-inch long section of guide which is enveloped by a solenoid. A signal pulse ten microseconds wide, with variable time delay after the dc discharge pulse, is sampled by a probe in a following section of guide, which can be mechanically rotated about the guide axis.

In Fig. 1 the rf electric field at the guide periphery is plotted as a function of angle for several values of magnetic field. In Fig. 2 the angle of rotation of the plane of maximum E -field is plotted as a function of magnetic field. The experimental conditions are

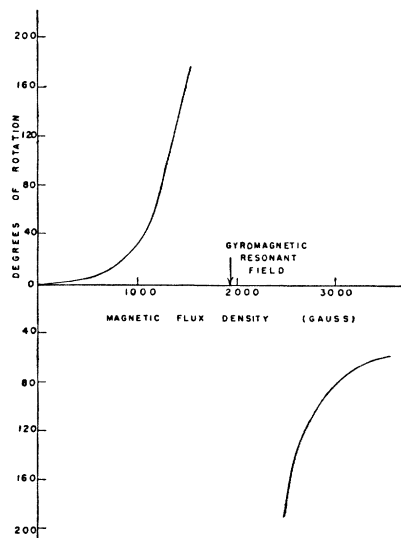


FIG. 2. Rotation of plane of maximum E -field vs magnetic field. The experimental conditions are the same as for Fig. 1.